

Effective persons identification using two- and three-dimensional finger knuckles

Abstract. Because of their high level of precision, biometric systems continue to attract the attention of several researchers. Different biometric traits have been investigated for use in security systems, such as fingerprints, faces, irises, palmprints, and knuckle prints. In most cases, bi-dimensional information is utilized. To achieve this aim, we have examined the performance of biometric identification systems based on a 3D-FKP database through five pre-trained networks such as AlexNet, VGG19, GoogleNet, ResNet50, and DenseNet201. The obtained experimental results illustrate the effectiveness of the suggested approach, with a high recognition rate and accuracy.

Streszczenie. Ze względu na wysoki poziom precyzji systemy biometryczne nadal przyciągają uwagę wielu badaczy. Zbadano różne cechy biometryczne pod kątem wykorzystania w systemach bezpieczeństwa, takie jak odciski palców, twarze, tęczówki, odciski dłoni i odciski kostek. W większości przypadków wykorzystuje się informacje dwuwymiarowe. Aby osiągnąć ten cel, zbadaliśmy wydajność systemów identyfikacji biometrycznej opartych na bazie danych 3D-FKP za pośrednictwem pięciu wstępnie wyszkolonych sieci, takich jak AlexNet, VGG19, GoogleNet, ResNet50 i DenseNet201. Uzyskane wyniki eksperymentalne ilustrują skuteczność zaproponowanego podejścia, przy wysokim współczynniku rozpoznawania i dokładności. (**Skuteczna identyfikacja osób za pomocą dwu- i trójwymiarowych kostek palców**)

Keywords: Biometrics, 2D/3D-FKP, Multimodal Identification, Deep learning, transfer learning, Fusion at level score.
Słowa kluczowe: biometria, identyfikacja osób, głębokie uczenie.

Introduction

The demand to automatically authenticate and identify individuals for numerous purposes, such as information secrecy, building access, and computer security, has dramatically increased in recent years. Biometrics is one of the most crucial and trustworthy techniques in this field. It involves identifying individuals based on their physiological traits, such as fingerprints [1, 2], iris [3, 4], retina [5], palmprints [6, 7], hand geometry [8], and face [9], or behavioral characteristics, such as voice [10], signature [11], and gesture [12].

Among many traits of biometric identification, Finger Knuckle Print (FKP) images [13, 14, 15] have gained popularity as biometric traits due to their accuracy, efficiency, and ease of acquisition. Recent trends have paid attention to 3D biometric information in addition to 2D intensity images because 3D images are more robust, invariant to illumination, and contain rich information. This trend has been studied in a number of biometric research projects, including 3D fingerprints [16, 17], 3D palmprints [18, 19, 20, 21], the 3D face [22, 23], the 3D ear [24, 25], and, most recently, 3D finger knuckle prints [26, 27, 28, 29, 30]. Because the 3D FKP is so new as a biometric identifier represented by a single database created by the Hong Kong Polytechnic University [31], it will be possible to offer numerous enhancements to the identification process.

Little work has been done using the 3D FKP database. Cheng and Kumar [26] were the first to use the contactless 3D FKP database in 2019 [31]. This database was collected from 130 different subjects in two sessions. In their paper, 3D depth data is converted into 2D images using the Frankot-Chellappa [32] or Poisson Solver [33] approaches. For feature extraction, they used the method of surface gradient derivatives. Additionally, Cheng and Kumar wrote three other papers. In the first paper [27], the authors have developed a highly effective matching approach that uses surface key points extracted from the 3D finger knuckle images using the reliable surface gradient derivative features. In this case, they used the extended database of 228 subjects, while 190 subjects contained two-session images. A comparative study with a publicly accessible 3D knuckle database reveals that their method is 23 times

faster and more accurate. Although their work focuses on 3D knuckle recognition, the method's performance on other publicly accessible databases with similar 3D biometric patterns (including 3D palmprints and 3D fingerprints) has verified the model's performance. In the second paper [28], the authors provided an additional study for 3D FKP recognition utilizing a novel deep neural network-based approach. This method simultaneously encodes and combines deep characteristics from several scales to create a more robust representation of deep features. Such collaborative feature representations are robustly matched to compensate for involuntary finger fluctuations during contactless imaging, utilizing an efficient alignment technique with a fully convolutional architecture. In the last paper [29], they could determine if a local shape was convex or concave along a given direction and encode the curvature information as binary templates of optimal sizes for future comparisons. Their solution may be applied to templates of various sizes and is superior to state-of-the-art technologies, as shown in the 3D knuckle database. In addition, they showed the generalizability of their method by testing it on 3D palmprint and finger vein datasets. Another work proposed by Chaa et al. [30]. This research proposes unimodal and multimodal (on score level fusion) contactless person identification systems based on 2D and 3D finger knuckle patterns. First, the Tan and Triggs normalization technique (TT) is applied to the depth of the 3D FKP image to obtain a TT 3D FKP image. Then, an innovative and effective technique, Monogenic Local Phase Quantization (MLPQ), is used to extract features from TT 2D and 3D FKP images. Experimental results utilizing the publicly available PolyU FKP dataset demonstrate that the given framework achieved significantly lower error rates and surpassed the state-of-the-art techniques.

The primary objective of any biometric identification system is to obtain a high identification rate with a low error rate. Recently, however, Convolutional Neural Networks (CNN) have demonstrated excellent performance in image classification [34]. Several specific biometric recognition challenges have been investigated as uses of this approach, such as fingerprint recognition [35], iris recognition [36] and face recognition [37], have been

studied as applications for this technology. The application of CNN to the 3D FKP identification system is highly motivated. This work aims to suggest unimodal and multimodal biometric identification systems based on 3D FKP images using convolutional neural networks with a transfer learning method through several celebrated pre-trained models of networks.

This paper's structure is as follows: Section 2 describes the proposed multimodal biometric system in which scores are fused at the matching level. The experimental setup and the findings from the evaluation of the proposed model's effectiveness are discussed in section 3. Section 4 concludes the paper and addresses significant recommendations for future study.

2. Proposed multimodal biometric identification system

As stated previously, we intend to create efficient biometric identification systems by applying deep transfer learning to 2D-FKP and 3D-FKP. As is the case with all biometric systems, the proposed systems consist of two phases: enrollment and identification. During the enrollment step, the pre-trained network performs feature extraction and classification to train the selected dataset. During the identification step, the identical technique is performed on the test dataset. Comparing the two datasets allows us to accept or reject an individual. The architecture of a multimodal biometric identification system is based on fusing the normalized scores of two or more unimodal systems at the matching score level. A diagram of the proposed multimodal biometric system based on 2D and 3D FKP and deep transfer learning is presented in Fig. 1.

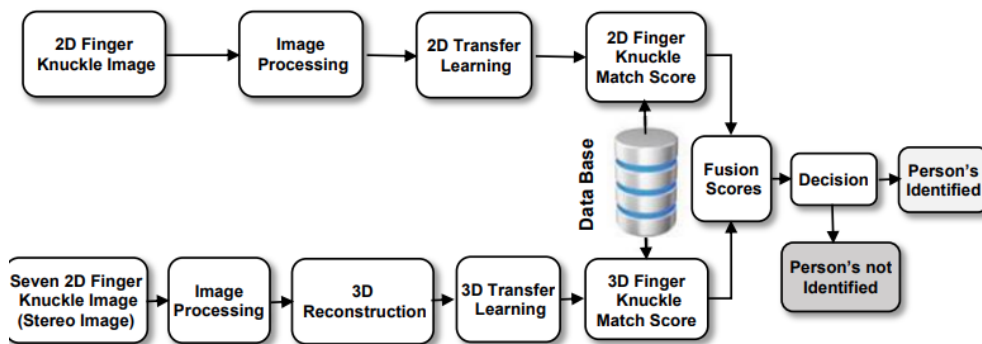


Fig.1. The proposed multimodal biometric system's architecture.

2.1. Pre-processing

To find the knuckle pattern region, a fixed-size rectangular window is put on the horizontal and vertical axes of the edge-detected image. Like in [38], the window's edge pixels are computed. The maximum number of edge pixels in the sliding window is used to segment a fixed region of interest from the image. The 3D segmented image will then be used as input for the 3D reconstruction

2.2. 3D reconstruction

The 3D depth information or the normal surface vectors has been acquired using a photometric stereo approach for the 3D imaging. The biometric imaging device consists of a camera, seven evenly distributed illuminations, a control circuit and a computer. In order to convert them to information of images, we used the Poisson solver [33].

2.3. Transfer learning

In order to create an efficient identification biometric system using 3D-KP images, we will propose to use famous networks based on transfer learning with fine-tuning and data augmentation [39, 40]. It entails taking features learned from one problem and applying them to a new, similar problem. Transfer learning is typically employed when the dataset contains insufficient information to train a full-scale model from scratch. In the context of deep learning, transfer learning is most often seen as the following workflow:

- Use previously trained model layers.
- Freeze them to prevent any information they contain from being destroyed during future training rounds.
- Add new trainable layers on top of the frozen layers. On a new dataset, the old features in predictions will be changed.
- Train the new layers on the dataset.

Fine-tuning is the last step. It involves unfreezing the built model (or just a part of it) and retraining it on the new data with a very low learning rate. Slowly adjusting the already-trained features to the new data could lead to significant improvements. For example, in the AlexNet network used in our work, the last three layers are replaced by an FC layer, a softmax layer, and an output layer, as seen in Fig. 2.

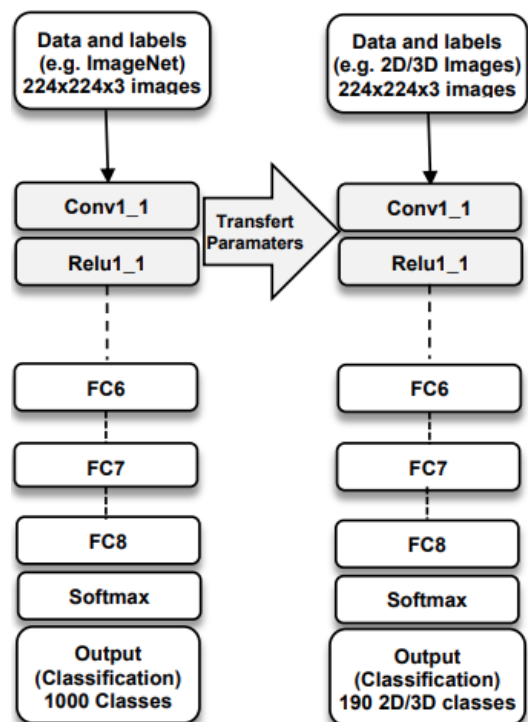


Fig. 2: Transfer learning using AlexNet network.

2.4. Matching and fusion scores

The match score measures feature vector similarity between the test (input) and training (model). When all match scores are compared, the template with the highest similarity score is shown to be the one with the highest match score. In score-level fusion, the match scores generated by various biometric systems are combined to determine a person's identity. Fusion at this level is the most frequently described strategy in the biometric literature because match scores are so simple to obtain and process. However, such a method only makes sense when the matchers' scores are comparable. Before using fusion procedures, the scores must be normalized to produce a common range of values in multimodal systems. Among several standardization methods, we have chosen to use the min-max method, which is simple and effective. The following equation expresses it [39]:

$$(1) \quad \hat{S}_i = \frac{S_i - \min(S_i)}{\max(S_i) - \min(S_i)}$$

While the vector \hat{S}_i contains the normalized scores of the modality i the vector S_i includes all the scores determined between the test and all the stored feature vectors. At this level, a variety of fusion rules can be applied. We will use the sum fusion rule because it is a simple and effective way to calculate fusion scores. It is expressed as follows [39]:

$$(2) \quad S_k = \sum_{i=1}^N \hat{S}_{ki}$$

Where S_k denotes the matching score of the k^{th} user's i^{th} biometric trait.

3. Experimental Results and Discussion

To evaluate the performance of the proposed 3D finger knuckle recognition framework, we present experimental results utilizing a recent publicly accessible 3D finger knuckle database. Furthermore, a comparative analysis with other studies validates the efficacy of our approach.

3.1. Contactless 3D Finger Knuckle Database

The Hong Kong Polytechnic University 3D FKP Database [28] was used to evaluate the performance of the proposed CNN-based identification systems. The HKPolyU 3D FKP database is a two-phase database containing 2D FKP and 3D FKP images [26]. It was acquired using a photometric stereo approach for 3D imaging. The biometric imaging device consists of a camera, seven evenly distributed lights, a control circuit, and a computer. The database was obtained from 228 different persons. Among the 228 persons, 190 have 2 sessions. The rest have a single session. six forefinger 2D knuckle images and six middle finger 2D knuckle images for each person in each session. However, there are 7 stereo photometric images for each 3D image. Therefore, forty-two photometric stereo 3D forefinger images and forty-two photometric stereo 3D middle finger images are available for each person in each session. The 3D depth information is converted by Poisson Solver [35] to a 2D image, which is a well-known technique for reconstructing the depth map while resolving the integrability issue. The Poisson Solver method produces a good visual outcome that approximates the natural knuckle patterns. Fig. 3 illustrates some sample images from this database.

Two databases are required to develop a 3D-FKP recognition application: one for training and the other for testing. However, there is no rule to determine this split quantitatively. It often results from a compromise, considering the amount of data available and the time to perform the learning. In the series of test, we carried out, we took the odd six images for training and even six for

testing for both sessions of 190 subjects. This evaluation protocol gives 215460 ($190 \times 189 \times 6$) imposter comparison scores and 1140 (190×6) genuine comparison scores.

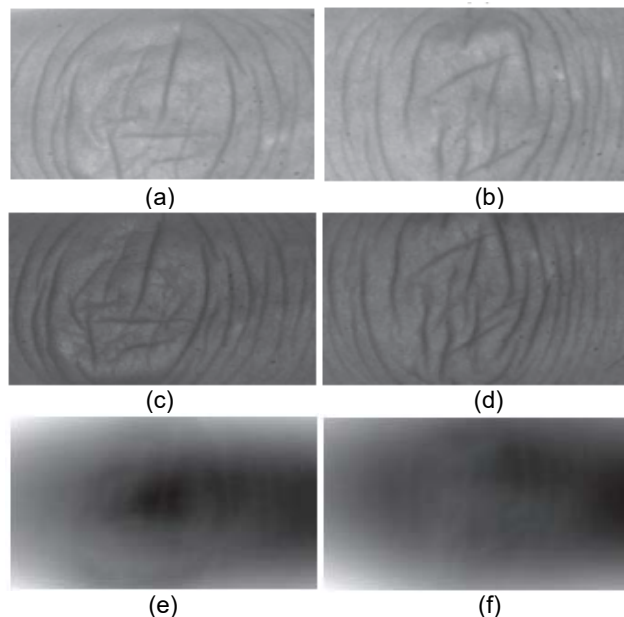


Fig. 3: Sample images from the database, first line: forefinger, second line: Middle finger, (a)/(b) 2D first session, (c)/(d) 2D second session, (e)/(f) 3D with Poisson solver.

3.2. Evaluation metrics

Evaluation of biometric identification systems can be done either by open-set or closed set identification modes. The first one does not guarantee the person's existence to be identified in the database, whereas in the second mode, it is presumed that the person exists. The following criteria can measure the performance of a biometric identification system for open-set identification [40]:

- The False Rejection Rate, or FRR, represents the percentage of persons who should be accepted, but the system rejects them. The following equation illustrates it.

$$(3) \quad FRR(\%) = \frac{\text{Number of rejected genuine (FR)}}{\text{Total number of genuine access}}$$

- The False Acceptance Rate, or FAR, represents the percentage of persons who should not be accepted, but the system accepted them. The following equation illustrates it.

$$(4) \quad FAR(\%) = \frac{\text{Number of accepted imposter (FA)}}{\text{Total number of imposter access}}$$

- The Equal Error Rate, or EER, represents the percentage where the false acceptance and rejection rates are equal ($FAR = FRR$). It constitutes an optimal compromise between false rejections and false acceptances.

Consequently, we may plot the Receiver Operating Characteristics (ROC) curve, representing the FRR versus the FAR.

To assess a biometric identification system's accuracy performance in closed-set identification, we employ the Cumulative Matching Characteristic (CMC) curve. It displays the ranking of individual templates depending on the percentage of matches. Two criteria are linked with this curve. The rank of Perfect Rate (RPR), which is defined as the rank at which the identification rate attempts 100%, and Rank-One Recognition (ROR), which is defined as the percentage of persons recognized by the system as a function of a variable "rank." The following equation determines it:

$$(5) \quad ROR(\%) = \frac{N_i}{N} \times 100$$

Where N_i represents the number of images successfully assigned to the correct identity, and N represents the total number of images attempting to assign an identity.

3.3. Adjusting Network Parameters

To construct effective biometric identification systems, we must carefully select the ideal parameters depending on the goal of the recognition performance. Therefore, before presenting our results, we must adapt and tune the parameters of the pre-trained networks to the dataset we used. First, the image size for inputs to the pre-trained networks is 227×227 for the AlexNet network and 224×224 for the VGG19, GoogleNet, and ResNet50 networks. So, our images need to be resized from 249×212 to these sizes when they enter the network. Also, our images are grayscale, so we need to convert them to color images. Finally, to increase the new database size and the trained network's adaptability and limit the overfitting problem, we rotate the images from minus ten to ten degrees, using a one-degree step for data augmentation.

Freezing some layers during transfer learning's fine-tuning can reduce computation time, albeit at the expense of accuracy when the new dataset is considerably different from the training dataset. In our case, more layers of adjustment may be required. In this study, we kept all of the pre-trained network layers. When developing a model with transfer learning, it is best to first test optimizers to acquire minimal bias and good results in the training set and then seek regularizers if overfitting is observed in the test set. Transfer learning requires a low learning rate for the selection of hyperparameters in order to take advantage of the pre-trained model weights. This choice of the optimizer (SGD, Adam, or RMSprop) will affect the number of epochs required to train a model successfully. So, after several experiments, we tested our identification systems with the SGD optimization method and tuned the learning rate to 0.001, the number of epochs to 50, and the batch size to 128.

3.4. Experimental results

We divided our experimental study into three parts. The first part will be devoted to the unimodal identification results. On the other hand, the second part will be for the multimodal identification results. Finally, in the last part, we will compare our work with the state-of-the-art. The different experiments of our biometric identification systems were executed on an experimental platform (HP Z8G4) with 64-bit Microsoft Windows 10, an Intel Xeon Silver 4108 processor, 96GB of RAM, and a GPU (GeForce RTX 2080Ti, GeForce RTX 3090).

3.4.1. Unimodal biometric identification system performance

After selecting the hyperparameters of each pre-trained network (AlexNet, VGG19, GoogleNet, ResNet50, and DenseNet201), the systems' performances are based on the four modalities (2D/3D forefinger, 2D/3D middle finger) were evaluated. Table 1 shows the test results in the two identification modes: open-set and closed-set. Figures Fig. 4 and Fig. 5 show the ROC curves and the CMC curves of the results found previously. Thus, in the case of open-set identification mode, the table shows that 3D images offer better results in terms of the EER than 2D. This is because 3D images have low variability (Fig.4) compared to 2D images, which allows good identification even at low resolution. The VGG19, ResNet50, and DenseNet201 networks can achieve a perfect result (0.0000% of EER) for

3D images. For 2D images, the ResNet50 and the DenseNet201 networks give excellent results.

Table 1: Performance of the unimodal biometric identification system based on five pre-trained networks.

Network	Modality	Dim	Accuracy		
			EER (%)	ROR (%)	RPR
AlexNet	Forefinger	2D	0.6838	94.6491	118
		3D	0.0083542	99.4737	2
	Middle finger	2D	0.5057	95.3509	42
		3D	0.0027847	99.2105	2
VGG19	Forefinger	2D	0.5363	96.0526	67
		3D	0.0000	100	1
	Middle finger	2D	0.4385	96.6667	27
		3D	0.0000	100	1
GoogleNet	Forefinger	2D	0.5670	95.9649	30
		3D	0.0055694	98.9474	3
	Middle finger	2D	0.5730	95.5263	34
		3D	0.0027847	99.4737	2
ResNet50	Forefinger	2D	0.4398	96.9298	53
		3D	0.0000	100	1
	Middle finger	2D	0.4002	96.3158	17
		3D	0.0000	100	1
DenseNet 201	Forefinger	2D	0.2631	97.0175	36
		3D	0.0000	100	1
	Middle finger	2D	0.4385	96.8421	102
		3D	0.0000	100	1

Indeed, these two networks are ranked among the best feature extraction networks. Similarly, the results obtained for the closed set identification mode also illustrate that 3D images improve identification performance compared to 2D images. This gives a very good impression of the importance of including this component in the identification operation to improve its accuracy. In this case, it can make the biometric system more resilient to spoofing attacks.

3.4.2. Multimodal biometric identification system performance

To improve the performance of our biometric identification systems, we combine two modalities (2D and 3D) of a finger for a single user at a score level using sum rule fusion. The fusion will be between Forefinger/Middle Finger 2D and Forefinger/Middle Finger 3D for the AlexNet and GoogleNet networks. The outcomes of these fusions are listed in Table 2.

The effectiveness of the multimodal identification system is assessed through a comparison with the 2D and 3D components of the unimodal system. For the 2D component, the decrease in the values of the EER and the increase in the ROR values of the multimodal system are remarkable for the two fingers (Forefinger and Middle finger) and the two networks (AlexNet and GoogleNet). For example, for the AlexNet network, the diminution of the EER is equal to 0.6802% and 0.5029% for the two fingers, the Forefinger and Middle finger, respectively. The ROR increase is 5.2332% and 4.5614% for both fingers. On the other hand, for the GoogleNet network, the EER decrease is 0.5670% and 0.5730% for Forefinger and Middle finger, respectively. Thus, for the ROR increase, we obtained 4.0351% and 4.4737%.

For the 3D component, the difference with the multimodal system is illustrated in Figures Fig. 6 and Fig.7. These figures sketch the histograms representing the EER and the ROR for the Forefinger and the Middle finger, respectively. Based on Table 2 and the Figures Fig.6 and Fig.7, the difference between the multimodal identification system and the 3D part of the unimodal identification system is not very big. A perfect result with an EER of 0.0000%, a ROR of 100%, and an RPR of 1 was obtained by the Google Net network.

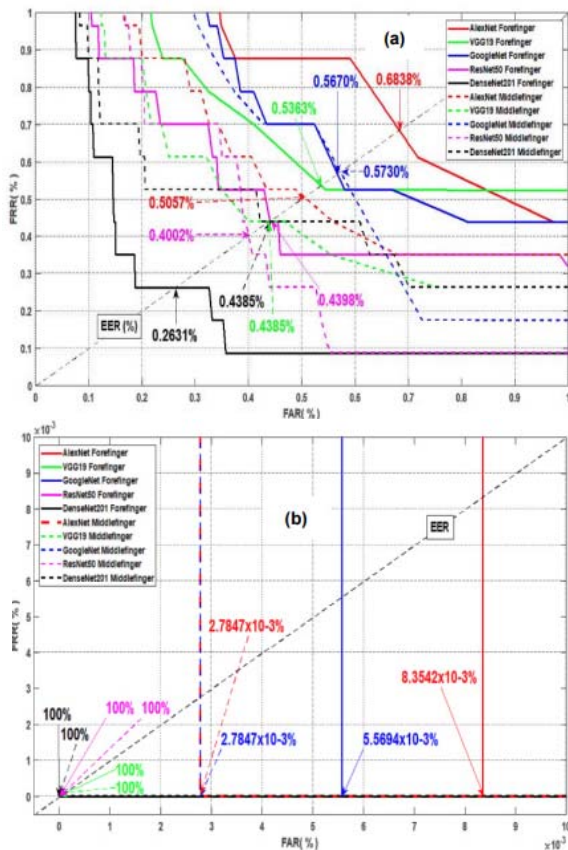


Fig. 4. ROC curves of unimodal biometric identification systems, (a) 2D images, (b) 3D images.

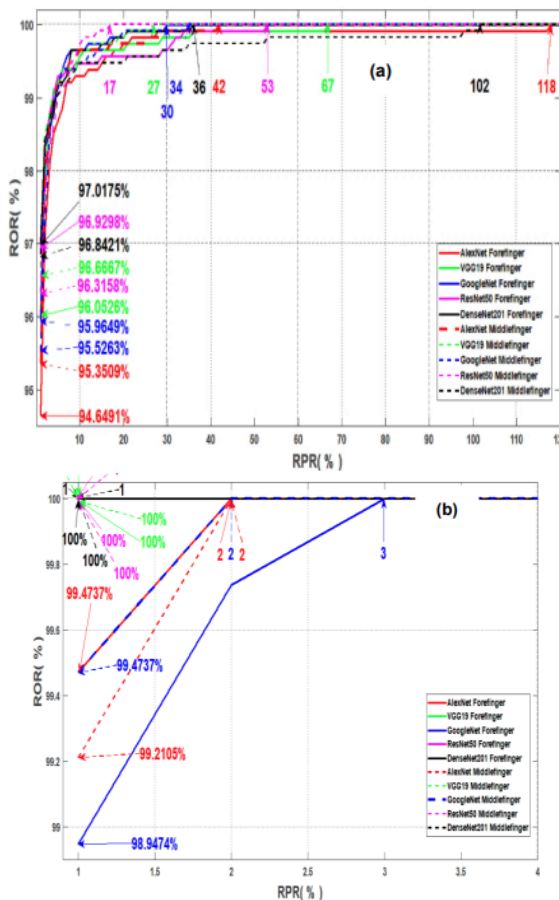


Fig. 5. CMC curves of unimodal biometric identification systems, (a) 2D images, (b) 3D images.

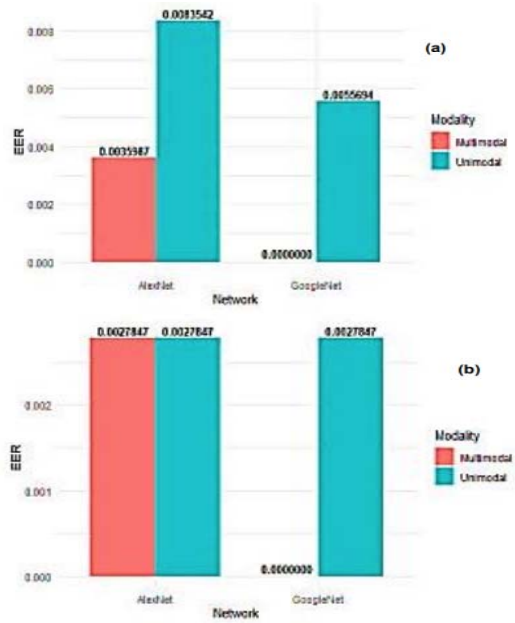


Fig. 6. Comparison between unimodal and multimodal EER, (a) Forefinger, (b) Middle finger.

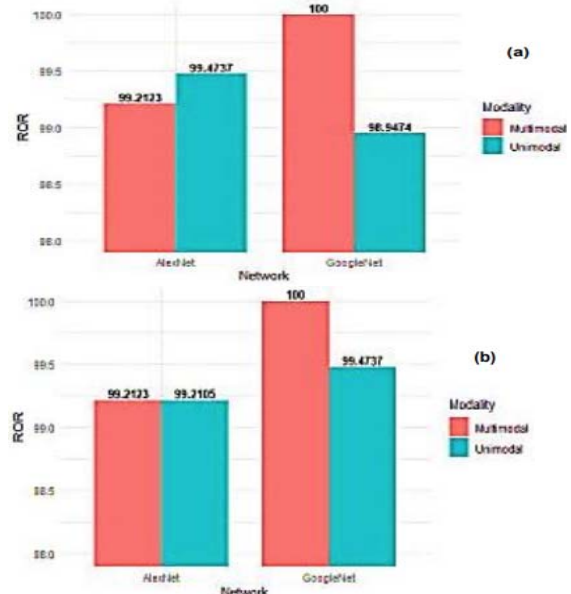


Fig. 7. Comparison between unimodal and multimodal ROR, (a) Forefinger, (b) Middle finger.

Table 2: Performance of the multimodal biometric identification system.

Modality	Fusion	Accuracy		
		EER (%)	ROR (%)	RPR
Forefinger	AlexNet 2D/AlexNet 3D	0.0035987	99.9123	2
Middle finger	AlexNet 2D/AlexNet 3D	0.0027847	99.9123	2
Forefinger	GoogleNet 2D/GoogleNet 3D	0.0000	100	1
Middle finger	GoogleNet 2D/GoogleNet 3D	0.0000	100	1

The fusion of modalities has improved the results. This proves that multimodal identification brings an improvement to the recognition systems. To further improve the performance of our multimodal identification system with the AlexNet network, we propose to fuse the score of the DenseNet201 2D network with the AlexNet 3D network since it gave the best results for 2D images. The results are shown in Table 3. In this case, the results have improved, and a perfect result has been reached.

Table 3: Performance of the proposed multimodal biometric identification system.

Modality	Fusion	Accuracy		
		EER (%)	ROR (%)	RPR
Forefinger	DenseNet201 2D/AlexNet 3D	0.0000	100	1
Middle finger	DenseNet201 2D/AlexNet 3D	0.0000	100	1

Table 4: Comparison with the state-of-the-art.

Identification System	Fingers	Work	Nbr of persons	ROR (%)	EER (%)
Uni-modal	2D-Forefinger	Cheng et al., [26]	105	89.5	10.2
		Chaa et al., [30]	105	96.03	1.77
		Ours	190	97.01	0.26
	2D-Middle finger	Chaa et al., [30]	105	96.98	0.82
		Chaa et al., [30]	190	96.84	0.43
	3D-Forefinger	Cheng et al., [26]	105	88.8	9.6
		Cheng et al., [28]	190	96.00	2.4
		Chaa et al., [30]	105	97.30	1.1
		Ours	190	100	0.00
	3D-Middle finger	Chaa et al., [30]	105	98.48	1.11
Ours		190	100	0.00	
Multi-modal	Forefinger (2D and 3D)	Cheng et al., [26]	105	90.35	8.7
		Chaa et al., [30]	105	97.46	0.79
		Ours	190	100	0.00
	Middle finger (2D and 3D)	Chaa et al., [30]	105	98.57	0.32
		Ours	190	100	0.00
	All finger (2D and 3D)	Chaa et al., [30]	105	99.52	0.16

3.4.3. Comparative study

To carry out a more in-depth evaluation to show the effectiveness of the systems proposed in this work, we have conducted a comparison with the state-of-the-art methods, in particular [26, 28, 30]; the results are shown in Table 4. These comparisons are made in the unimodal and multimodal systems and with both modes, i.e., in the open-set identification mode with the EER and the closed set identification mode with ROR performances. From Table 4, we can conclude that our biometric identification systems outperform the state-of-the-art methods with a higher ROR and lower error.

4. Conclusion

This paper developed contactless 3D finger-knuckle identification systems based on deep transfer learning. Two types of biometric systems have been proposed: unimodal and multimodal. Our experimental results using a publicly available contactless 3D finger knuckle database demonstrate the effectiveness of our proposed approach for both types. Also, the proposed identification scheme outperformed other schemes recently proposed. We aim to use visual transforms in the future to improve this work, either for person recognition or other applications such as spoof attacks.

Authors

Dr. Faouzi Bouchareb¹, Dr. Djamel Samai², Dr. Maarouf Korichi², Dr. Abdallah Meraoumia³ and Dr. Abderrazak Lachouri^{*1}

¹ Automatic Laboratory, Department of Electrical Engineering, University of 20 August 1955, Skikda Algeria.

² Univ Ouargla, Fac. des nouvelles technologies de l'information et de la communication. Lab. de Génie Electrique (LAGE), 30000, Ouargla, Algeria.

³ Laboratory of Mathematics, Informatics and Systems (LAMIS), Larbi Tebessi University, 12002 Tebessa, Algeria.

E-mails: bouchareb.faouzi@gmail.com, samai.djamel@univ-ouargla.dz, korichi.maarouf@univ-ouargla.dz, ameraoumia@gmail.com, alachouri@yahoo.fr

*Corresponding author: Abderrazak Lachouri alachouri@yahoo.fr

REFERENCES

- [1] Anil Jain, Arun Ross, and Salil Prabhakar. Fingerprint matching using minutiae and texture features. In *Proceedings 2001 International Conference on Image Processing* (Cat. No. 01CH37205), vol 3, pages 282–285. IEEE, 2001.
- [2] Anil K Jain, Jianjiang Feng, and Karthik Nandakumar. Fingerprint matching. *Computer*, 43(2):36–44, 2010.
- [3] John Daugman. New methods in iris recognition. *IEEE Trans on Systems, Man, and Cybernetics, Part B (Cybernetics)*, 37(5):1167–1175, 2007.
- [4] Kien Nguyen, Clinton Fookes, Raghavender Jillela, Sridha Sridharan, and Arun Ross. Long range iris recognition: A survey. *Pattern Recognition*, 72:123–143, 2017.
- [5] Halvor Borgen, Patrick Bours, and Stephen D Wolthusen. Visible-spectrum biometric retina-recognition. In *2008 International Conference on Intelligent Information Hiding and Multimedia Signal Processing*, pages 1056–1062. IEEE, 2008.
- [6] Adams Kong, David Zhang, and Mohamed Kamel. A survey of palmprint recognition. *pattern recognition*, 42(7):1408–1418, 2009.
- [7] Dexing Zhong, Xuefeng Du, and Kuncai Zhong. Decade progress of palmprint recognition: A brief survey. *Neurocomputing*, 328:16–28, 2019.
- [8] Nidhi Saxena, Vipul Saxena, Neelesh Dubey, and Pragya Mishra. Hand geometry: A new method for biometric recognition. *International Journal of Soft Computing and Engineering (IJSCE)*, 2(6):2231–2307, 2013.
- [9] Harry Wechsler, Jonathon P Phillips, Vicki Bruce, Francoise Fogelman Soulie, and Thomas S Huang. *Face recognition: From theory to applications*, volume 163. Springer Science & Business Media, 2012.
- [10] Attila Andics, James M McQueen, Karl Magnus Petersson, Viktor G'ál, G'abor Rudas, and Zolt'an Vidny'anszky. Neural mechanisms for voice recognition. *Neuroimage*, 52(4):1528–1540, 2010.
- [11] Ali Karouni, Bassam Daya, and Samia Bahlak. Ofine signature recognition using neural networks approach. *Procedia Computer Science*, 3:155–161, 2011.
- [12] Sushmita Mitra and Tinku Acharya. Gesture recognition: A survey. *IEEE Transactions on Systems, Man, and Cybernetics, Part C (Applications and Reviews)*, 37(3):311–324, 2007.
- [13] Lin Zhang, Lei Zhang, David Zhang, and Hailong Zhu. Ensemble of local and global information for finger-knuckle-print recognition. *Pattern recognition*, 44(9):1990–1998, 2011.
- [14] Yikui Zhai, He Cao, Lu Cao, Hui Ma, Junyin Gan, Junying Zeng, Vincenzo Piuri, Fabio Scotti, Wenbo Deng, Yihang Zhi, et al. A novel finger-knuckle-print recognition based on batchnorm-malized cnn. In *Chinese conference on biometric recognition*, pages 11–21. Springer, 2018.
- [15] A Zohrevand, Z Imani, and M Ezoji. Deep convolutional neural network for finger-knuckle-print recognition. *International Journal of Engineering*, 34(7):1684–1693, 2021.
- [16] Feng Liu, David Zhang, and Linlin Shen. Study on novel curvature features for 3d fingerprint recognition. *Neurocomputing*, 168:599–608, 2015.
- [17] Xuefei Yin, Yanming Zhu, and Jiankun Hu. 3d fingerprint recognition based on ridge-valley-guided 3d reconstruction and 3d topology polymer feature extraction. *IEEE transactions on pattern analysis and machine intelligence*, 43(3):1085–1091, 2019.
- [18] Wei Li, Lei Zhang, and David Zhang. Three dimensional palmprint recognition. In *2009 IEEE International Conference on Systems, Man and Cybernetics*, pages 4847–4852. IEEE, 2009.
- [19] Lin Zhang, Ying Shen, Hongyu Li, and Jianwei Lu. 3d palmprint identification using block-wise features and collaborative representation. *IEEE transactions on pattern analysis and machine intelligence*, 37(8):1730–1736, 2014.
- [20] Djamel Samai, Khaled Bensid, Abdallah Meraoumia, Abdelmalik Taleb-Ahmed, and Mouldi Bedda. 2d and 3d palmprint recognition using deep learning method. In *2018 3rd International*

- Conference on Pattern Analysis and Intelligent Systems (PAIS)*, pages 1–6. IEEE, 2018.
- [21] Mourad Chaa, Zahid Akhtar, and Abdelouahab Attia. 3d palmprint recognition using unsupervised convolutional deep learning network and svm classifier. *IET Image Processing*, 13(5):736–745, 2019.
- [22] Alize Scheenstra, Arnout Ruifrok, and Remco C Veltkamp. A survey of 3d facerecognition methods. In *International Conference on Audio-and Video-based Biometric Person Authentication*, pages 891–899. Springer, 2005.
- [23] Song Zhou and Sheng Xiao. 3d face recognition: a survey. *Human-centric Computing and Information Sciences*, 8(1):1–27, 2018.
- [24] Hui Chen and Bir Bhanu. Human ear recognition in 3d. *IEEE Transactions on Pattern Analysis and Machine Intelligence*, 29(4):718–737, 2007.
- [25] Iyyakutti Iyappan Ganapathi, Syed Sadaf Ali, Ngoc-Son Vu, Surya Prakash, and Naoufel Werghi. A survey of 3d ear recognition techniques. *ACM Computing Surveys (CSUR)*, 2022.
- [26] Kevin HM Cheng and Ajay Kumar. Contactless biometric identification using 3d fnger knuckle patterns. *IEEE transactions on pattern analysis and machine intelligence*, 42(8):1868–1883, 2019.
- [27] Kevin HM Cheng and Ajay Kumar. Efcient and accurate 3d fnger knuckle matching using surface key points. *IEEE Transactions on Image Processing*, 29:8903–8915, 2020.
- [28] Kevin HM Cheng and Ajay Kumar. Deep feature collaboration for challenging 3d fnger knuckle identification. *IEEE Transactions on Information Forensics and Security*, 16:1158–1173, 2020.
- [29] Kevin HM Cheng and Ajay Kumar. Accurate 3d fnger knuckle recognition using auto-generated similarity functions. *IEEE Transactions on Biometrics, Behavior, and Identity Science*, 3(2):203–213, 2021.
- [30] Mourad Chaa, Zahid Akhtar, and Abdehai Lati. Contactless person recognition using 2d and 3d fnger knuckle patterns. *Multimedia Tools and Applications*, 81(6):8671–8689, 2022.
- [31] Kumar. FKP 3D database. <https://www4.-comp.polyu.edu.hk/~csajayk/3DKnuckle.htm>, 2019 (accessed September 30, 2022).
- [32] Robert T. Frankot and Rama Chellappa. A method for enforcing integrability in shape from shading algorithms. *IEEE Transactions on pattern analysis and machine intelligence*, 10(4):439–451, 1988.
- [33] Tal Simchony, Rama Chellappa, and Min Shao. Direct analytical methods for solving poisson equations in computer vision problems. *IEEE transactions on pattern analysis and machine intelligence*, 12(5):435–446, 1990.
- [34] Farhana Sultana, Abu Sufan, and Paramartha Dutta. Advancements in image classification using convolutional neural network. In *2018 Fourth International Conference on Research in Computational Intelligence and Communication Networks (ICRCICN)*, pages 122–129. IEEE, 2018.
- [38] Bhavesh Pandya, Georgina Cosma, Ali A Alani, Aboozar Taherkhani, Vinayak Bharadi, and TM McGinnity. Fingerprint classification using a deep convolutional neural network. In *2018 4th International Conference on Information Management (ICIM)*, pages 86–91. IEEE, 2018.
- [39] Maram G Alaslani. Convolutional neural network based feature extraction for iris recognition. *International Journal of Computer Science & Information Technology (IJCSIT) Vol, 10*, 2018.
- [40] Rondik J Hassan, Adnan Mohsin Abdulazeez, et al. Deep learning convolutional neural network for face recognition: A review. *International Journal of Science and Business*, 5(2):114–127, 2021.
- [41] Ajay Kumar and Ch Ravikanth. Personal authentication using fnger knuckle surface. *IEEE Transactions on Information Forensics and Security*, 4(1):98–110, 2009.
- [42] Waziha Kabir, M Omair Ahmad, and MNS Swamy. Normalization and weighting techniques based on genuine-impostor score fusion in multi-biometric systems. *IEEE Trans on Information Forensics and Security*, 13(8):1989–2000, 2018.
- [43] Ted Dunstone and Neil Yager. Biometric system and data analysis: Design, evaluation, and data mining. Springer, 2009.